Research Square

Preprints are preliminary reports that have not undergone peer review.
They should not be considered conclusive, used to inform clinical practice,
or referenced by the media as validated information.

RNA-Seq Analysis Reveals the Regulation of Fecundity by Aldehyde Oxidase TcAOX1 in Tribolium castaneum

Shanshan Gao
Anyang Institute of Technology
Can Zhou
Anyang Institute of Technology
ZuPei Yi
Anyang Institute of Technology
Miao Wang
Anyang Institute of Technology
Kunpeng Zhang
zhangkunpengag@163.com

Anyang Institute of Technology

Research Article

Keywords: Aldehyde oxidase, RNA-Seq, Fecundity, Tribolium castaneum

Posted Date: November 11th, 2026

DOI: https://doi.org/10.21203/rs.3.rs-10637541/v1

License: This work is licensed under a Creative Commons Attribution 4.0 International License.
Read Full License

Additional Declarations: No competing interests reported.

RNA-Seq Analysis Reveals the Regulation of Fecundity by Aldehyde Oxidase *TcAOX1* in *Tribolium castaneum*

Shanshan Gao [1, 2], Can Zhou [1], ZuPei Yi [1], Miao Wang [1], Kunpeng Zhang [1]*

[1] Department of Food and Bioengineering, Anyang Institute of Technology, Anyang, Henan, 455000, China

[2] Taihang Mountain, Forest Pests Observation and Research Station of Henan Province, Linzhou, 456550, China

*Corresponding author:

Kunpeng Zhang, Department of Food and Bioengineering, Anyang Institute of Technology, Anyang, Henan, China. E-mail address: zhangkunpengag@163.com

Abstract

Aldehyde oxidases (AOXs) play important roles in insects, including involvement in the detoxification of xenobiotics and the degradation of odorant signals. Previous studies have suggested that *TcAOX1* may be involved in regulating the reproductive process of *Tribolium castaneum.* However, the precise mechanism by which *TcAOX1* affects reproduction in *T. castaneum* remains unclear. Therefore, in this study, we established a control group and a *TcAOX1* knockdown group, each with three biological replicates. Following the knockdown of *TcAOX1* expression, RNA-Seq was performed. Differentially expressed genes (DEGs) were analyzed using Gene Ontology (GO) and Kyoto Encyclopedia of Genes and Genomes (KEGG) enrichment analyses for functional annotation. In the GO analysis, eight genes were enriched in the catalytic activity term, and six genes were enriched in the metabolic process term. In the KEGG analysis, enrichment was observed across five categories: cellular processes, environmental information processing, human diseases, metabolism, and organismal systems. Following *TcAOX1* knockdown, the expression of the aforementioned enriched genes—including *serine protease P145*, *serine protease P147*, *serine protease P41*, and *carboxypeptidase A*—was downregulated. Additionally, the expression of *cuticlin-2*, a cuticle protein gene implicated in the reproduction of *T. castaneum*, was also reduced. The downregulation of these genes may contribute to decreased oviposition rate and impaired embryonic development in *T. castaneum*. These findings suggest that *TcAOX1* may influence reproduction in *T. castaneum* by modulating the expression of the above genes. This study provides a theoretical basis for research on reproduction in *T. castaneum* and offers new insights for the development of green pest control strategies against this species.

Keywords: Aldehyde oxidase, RNA-Seq, Fecundity, *Tribolium castaneum,*

Introduction

Aldehyde oxidases (AOXs) are a class of molybdo-flavoenzymes widely distributed in animals, plants, and microorganisms, and share structural homology with xanthine oxidoreductase in an evolutionary context(Gao, Liu, et al., 2025; Terao et al., 2016). Aldehyde oxidases (AOXs) catalyze the oxidation of aldehydes to their corresponding carboxylic acids, with concomitant production of reactive oxygen species (ROS). They possess an exceptionally broad substrate spectrum, being capable not only of oxidizing aromatic and aliphatic aldehydes but also of hydroxylating a wide range of heteroaromatic compounds(Terao et al., 2016). In mammals, AOXs are primarily involved in drug metabolism and the detoxification of xenobiotics(Garattini, Fratelli, & Terao, 2009);In plants, they are involved in the synthesis of abscisic acid and indole-3-acetic acid (i.e., hormone biosynthesis pathways); in microorganisms, they are involved in ethanol metabolism.(Gao, Liu, et al., 2025).In insects, aldehyde oxidases serve dual functions in the detoxification of xenobiotics and the degradation of odorant signals, including the breakdown of pheromones. Previous studies have shown that *HarmAOX2* from the cotton bollworm, *Helicoverpa armigera*, is a candidate odorant-degrading enzyme (ODE) responsible for inactivating the sex pheromone components (Z)-11-hexadecenal and (Z)-9-hexadecenal(W. Xu & Liao, 2017).*AtraAOX2* from the navel orangeworm (*Amyelois transitella*) may be involved in the degradation of a diversity of aldehydes, including sex pheromones, plant-derived semiochemicals, and chemical cues for oviposition sites, as well as in protecting the insect's olfactory system from xenobiotics(Choo, Pelletier, Atungulu, & Leal, 2013);In the antennae of the tobacco hawkmoth *Manduca sexta*, aldehyde oxidase oxidizes aldehydes to carboxylic acids. This enzyme is secreted into the sensillum lymph and exhibits high affinity for the pheromone component *bombykal*. Its developmental expression pattern coincides with the adult olfactory sensitive period, suggesting that it is involved in modulating the adult's sensitivity to aldehyde odors(Rybczynski, Reagan, & Lerner, 1989);*GmelAOX2* and *GmelAOX3* from the greater wax moth, *Galleria mellonella*, play key roles in the metabolism of sex pheromone compounds and plant-derived aldehydes(Godoy, Arias, Venthur, Quiroz, & Mutis, 2022).Recombinant proteins *AtraAOX2*, *PxylAOX3*, and *BmAOX5* from *A. transitella*, *P. xylostella*, and *B. mori*, respectively, can degrade sex pheromones or plant-derived volatiles in vitro(Choo et al., 2013; Wang et al., 2021; Yandi Zhang et al., 2020).Current control strategies for *T. castaneum*, a globally widespread stored-product pest, include not only the application of insecticides but also pheromone-based trapping of insects(Barun Mangang, Loganathan,

Malemnganbi, & Induja, 2025),The inactivation of pheromone signals is closely associated with aldehyde oxidases(Pelletier et al., 2007).Furthermore, studies have shown that pheromone-degrading enzymes in insects, such as esterases and aldehyde oxidases, can terminate pheromone signals, thereby affecting insect reproduction(Chertemps et al., 2012; Rybczynski, Vogt, & Lerner, 1990). Our previous studies have shown that knockdown of the aldehyde oxidase gene *TcAOX1* in *T. castaneum* leads to a decrease in oviposition rate, while the hatching rate and the development of reproductive organs remain unchanged, suggesting that this gene may regulate fecundity through the inactivation of chemical signals(Yonglei Zhang et al., 2022).

In our previous studies, three aldehyde oxidase genes, *TcAOX1*, *TcAOX2*, and *TcAOX3*, were identified in *T. castaneum*. It was found that the transcripts of *TcAOX2* and *TcAOX3* were significantly induced upon exposure to mugwort essential oil, and that knockdown of their expression enhanced the susceptibility of *T. castaneum* to this essential oil. Furthermore, RNA-Seq analysis of late-instar larvae with *TcAOX2* and *TcAOX3* knockdown revealed that alterations in the expression of these two genes may affect the expression of various genes involved in metabolism, digestion, or immunity, thereby influencing the susceptibility of *T. castaneum* to external xenobiotics(Gao, Guo, et al., 2025; Gao, Liu, et al., 2025).In contrast to *TcAOX2* and *TcAOX3*, knockdown of *TcAOX1* expression resulted in reduced egg production in females, with no changes in the hatching rate or the development of reproductive organs(Yonglei Zhang et al., 2022).

However, the precise mechanism by which *TcAOX1* regulates reproduction in *T. castaneum* remains unclear. To further investigate this issue, the present study was designed with a control group and a *TcAOX1* treated group, each comprising three biological replicates. RNA interference (RNAi) was employed to knock down *TcAOX1* expression, followed by RNA sequencing (RNA-Seq) to identify differentially expressed genes (DEGs). Functional annotation and pathway enrichment analyses were performed using Gene Ontology (GO) and the Kyoto Encyclopedia of Genes and Genomes (KEGG). This study provides a theoretical foundation for research on reproduction in *T. castaneum* and offers new perspectives for the development of environmentally friendly pest management strategies against this species.

Materials and methods

Rearing of *Tribolium castaneum*

The *T. castaneum* strain used in this study (Georgia-1 strain) was obtained from Nanjing Normal University. The beetles were reared on a diet consisting of wheat flour and yeast powder mixed at a ratio of 19:1 . Both the diet and the beetles were kept in glass jars and placed in an incubator. The incubator was maintained at 30°C with a relative humidity of 40%, under a photoperiod of 14 h light : 10 h dark(Gao et al., 2021).

dsRNA Synthesis and Injection

Gene-specific primers for *TcAOX1* and *TcVER* (*T. castaneum vermilion*, GenBank accession No. AY052390) containing the T7 polymerase promoter recognition sequence were designed using Primer Premier 5.0 software for dsRNA synthesis. The PCR amplification system consisted of 0.4 μL each of forward and reverse primers (10 μM), 10 μL of 2× PrimeSTAR Mix, 8.2 μL of DEPC-treated H_2O, and 1 μL of cDNA. The PCR amplification program was as follows: initial denaturation at 94°C for 5 min, followed by 35 cycles of denaturation at 94°C for 30 s, annealing at 60°C for 30 s, and extension at 72°C for 2 min, with a final extension at 72°C for 7 min. The purified PCR products were used as templates for dsRNA synthesis using the T7 High-Yield Transcription Kit (Fermentas, Vilnius, Lithuania). The dsRNA was injected into late-instar larvae of *T. castaneum* between the penultimate and third abdominal segments from the posterior end using a Nanoject III injector (Drummond Scientific, Philadelphia, PA, USA). Each larva received an injection of 200 nL of solution containing 200 ng of dsRNA. Control larvae were injected with an equal volume of injection buffer (IB) or 200 ng of ds*VER*. Forty larvae were injected per group. On day 5 post-injection, three larvae from each group were collected to examine the expression of *TcAOX1*. All experiments were performed with three biological replicates.

RNA Extraction, Reverse Transcription, and RNA-Seq

On day 5 post-injection, six larvae were collected from each group: three were used for RNA extraction, and the remaining three were stored at −80°C for later use. Total RNA was extracted using TRIzol reagent (Vazyme, Nanjing, China) according to the manufacturer's instructions. RNA integrity was assessed by agarose gel electrophoresis, and RNA concentration and purity were measured using a NanoDrop 2000 spectrophotometer (Thermo Fisher Scientific, Wilmington, DE, USA). RNA samples that passed quality control were subjected to reverse transcription, and the resulting cDNA was stored

at −20°C for subsequent use. The remaining RNA was sent to the Beijing Genomics Institute (BGI, Shenzhen, China) for sequencing on the BGI platform. The raw sequence data have been deposited in the National Center for Biotechnology Information (NCBI) database under the following accession numbers: SAMN49032583, SAMN49032584, and SAMN49032585 for the *TcAOX1* samples, and SAMN48911764, SAMN48911765, and SAMN48911766 for the IB samples.

RNA-Seq Data Quality Control and Analysis

Raw sequencing data were subjected to quality control and filtering using SOAP-nuke (v.1.5.6) software. Reads containing adapters, reads with more than 5% unknown bases (N), and low-quality reads (defined as reads in which more than 20% of bases had a quality score < 15) were removed(X. Chen et al., 2018; Y. Chen et al., 2018).. The resulting clean reads were then aligned to the reference genome and the reference gene sequences using HISAT(Kim, Langmead, & Salzberg, 2015) and Bowtie2 (Langmead & Salzberg, 2012), respectively. Differentially expressed genes (DEGs) were identified using DESeq2 (v.1.4.5) (Love, Huber, & Anders, 2014)with the following criteria: $P \leq 0.05$ and $|\log_2(\text{fold change})| \geq 1.0$. The fold change was calculated as $\log_2$(FPKM of the ds*TcAOX1*-injected group) − $\log_2$(FPKM of the IB-injected group). FPKM (fragments per kilobase of transcript per million mapped reads) represents the normalized transcript abundance.

QPCR Validation of RNA-Seq Data

Quantitative real-time PCR(qPCR)was performed using SYBR Green Master Mix as the fluorescent dye. Each reaction mixture consisted of 0.25 μL each of forward and reverse primers (10 μM), 5 μL of 2× AceQ Universal SYBR qPCR Master Mix, 3.5 μL of ddH_2O, and 1 μL of cDNA. The thermal cycling program was as follows: initial denaturation at 95°C for 10 min, followed by 40 cycles of denaturation at 95°C for 15 s and annealing at 60°C for 60 s, and a final dissociation curve analysis consisting of 95°C for 15 s, 60°C for 60 s, and 95°C for 15 s. All qPCR reactions were performed on an ABI Q6 instrument (Applied Biosystems, Foster City, CA, USA). The *Tcrps3* gene (encoding ribosomal protein S3) was used as the internal reference gene, and the relative expression levels of target genes were calculated using the $2^{-}\Delta\Delta Ct$ method. The primers used for qPCR validation are listed in Table S1. All treatments and controls were performed with three biological replicates.

Table S1. Primer information

Gene	Sequence (5'-3')	Primer length (bp)	Product length (bp)
LOC664115-F	CCGGTGGTTACGATTGAAGA	20	154
LOC664115-R	ACTGGAAACATTGCGAAGGG	20	154
LOC656185-F	TTTGGTTTCGTTGCCTTTCA	20	158
LOC656185-R	GCACCGGATTTTTCTTTGTTTC	22	158
LOC661254-F	TTCCAGTGACAATGTAGTTCAAGTG	25	150
LOC661254-R	TTGGGGAGTGTGACTGGTTGA	21	150
LOC656929-F	AACTGGTGGAAAATCCCTCTTAT	23	204
LOC656929-R	CGGAACCACTGGCACCTTT	19	204
LOC655120-F	CCCCTTTGGGAGTTGGAGC	19	145
LOC655120-R	GGTCCCCAGAGCCCATCA	18	145
LOC656097-F	ATTCCCTTTTATAATTTCCCTTCG	24	154
LOC656097-R	GTTTAGTTGGTTGATTCCTGCG	22	154
LOC100141947-F	CTCCGCCAAACGACCAAA	18	229
LOC100141947-R	CCCGCATTAACTGCTTCCAC	20	229
LOC662042-F	CCTTAGGCATGTTTGGCTCTT	21	299
LOC662042-R	TTTCCCCCTCATTCGGTTC	19	299
LOC103312224-F	TAACAAGTGATGATGGTAAAAACGA	25	152
LOC103312224-R	ACCAGCATCACCACTGAATCC	21	152

Statistical Analysis

Statistical analyses were performed using SPSS statistical software (SPSS Inc., Chicago, IL, USA). Gene expression data and the means of RNAi-treated and control larvae were analyzed by one-way analysis of variance (ANOVA) followed by Fisher's least significant difference (LSD) multiple comparison test, as well as by Student's t-test where appropriate. All data are presented as mean ± standard error (SE), and error bars represent the SE of three biological replicates. A probability value of $P < 0.05$ was considered statistically significant, while $***P < 0.001$ were considered highly significant.

Results

Knockdown Efficiency of *TcAOX1*

RNA interference (RNAi) was employed to knock down the expression of *TcAOX1*. To confirm the effectiveness of this intervention, the expression level of *TcAOX1* was examined by qPCR. The expression of *TcAOX1* was reduced to 13% of that in the control group, corresponding to a knockdown efficiency of 87% (Fig. 1).

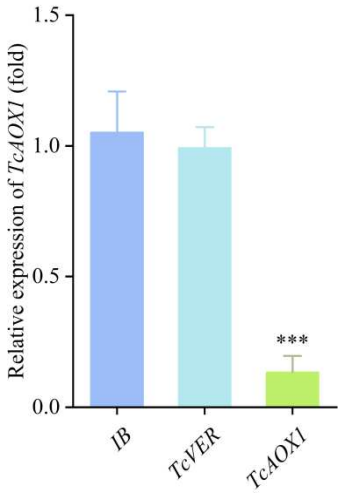


Fig. 1. Knockdown efficiency of *TcAOX1* as determined by qPCR..Student's t-test was used for statistical comparisons among insects injected with equal amounts of ds*TcVER* (*T. castaneum vermilion*, GenBank accession No. AY052390), IB (injection buffer, wild-type untreated), and ds*TcAOX1*. Data and error bars represent the mean ± standard error (SE) of three biological replicates. Three asterisks indicate a highly significant difference between the control and treated groups at $P < 0.001$.

RNA-Seq Data Quality Assessment

The raw sequencing reads were generated on the Illumina high-throughput sequencing platform. After quality control filtering and removal of invalid low-quality reads, high-quality clean reads were obtained for subsequent analyses (Table 1). The processed clean reads were then aligned to the *T. castaneum* reference genome and reference gene annotation. The alignment results showed that the reads were evenly distributed across both the reference genome and reference gene sequences, with uniquely mapping ratios exceeding 80% and 60%, respectively (Tables S2 and S3). In addition, the squared Pearson correlation coefficient (R^2) was calculated to evaluate the consistency among biological replicates, and all inter-sample R^2 values were above 0.7 (Fig. 2). Collectively, these results demonstrate that the RNA-Seq data generated in this study are of high quality and meet the

190 requirements for subsequent statistical analyses.

191 Table 1. Quality filtering statistics of the reads.

Sample Name	Total Raw Reads	Total Clean Reads	Total Clean Bases	Clean Reads Q20	Clean Reads Q30	Clean Reads Ratio
IB_1	54.18	44.94	6.74	97.59	92.02	82.95
IB_2	52.43	43.92	6.59	97.67	92.30	83.78
IB_3	50.68	43.97	6.60	97.51	91.70	86.77
ds*TcAOX1*_1	50.68	44.14	6.62	97.56	91.88	87.08
ds*TcAOX1*_2	45.45	40.50	6.07	97.16	90.60	89.11
ds*TcAOX1*_3	50.68	44.50	6.68	97.43	91.45	87.81

192

193 Table S2. Alignment statistics of clean reads mapped to the reference genome using HISAT.

Sample Name	Total clean Read	Total Mapping Genome Ratio	Uniquely Mapping Genome Ratio
IB_1	44.94	89.84	87.19
IB_2	43.92	89.86	87.59
IB_3	43.97	90.78	88.74
ds*TcAOX1*_1	44.14	91.17	89.41
ds*TcAOX1*_2	40.50	90.51	88.26
ds*TcAOX1*_3	44.50	90.15	88.10

194

195 Table S3. Alignment statistics of clean reads mapped to the reference gene sequences using Bowtie2.

Sample Name	Total clean Read	Total Mapping Gene Ratio	Uniquely Mapping Gene Ratio
IB_1	44.94	71.48	67.20
IB_2	43.92	70.68	67.41
IB_3	43.97	71.82	69.01
ds*TcAOX1*_1	44.14	72.06	69.72
ds*TcAOX*1_2	40.50	71.66	68.64
ds*TcAOX1*_3	44.50	70.81	68.39

196

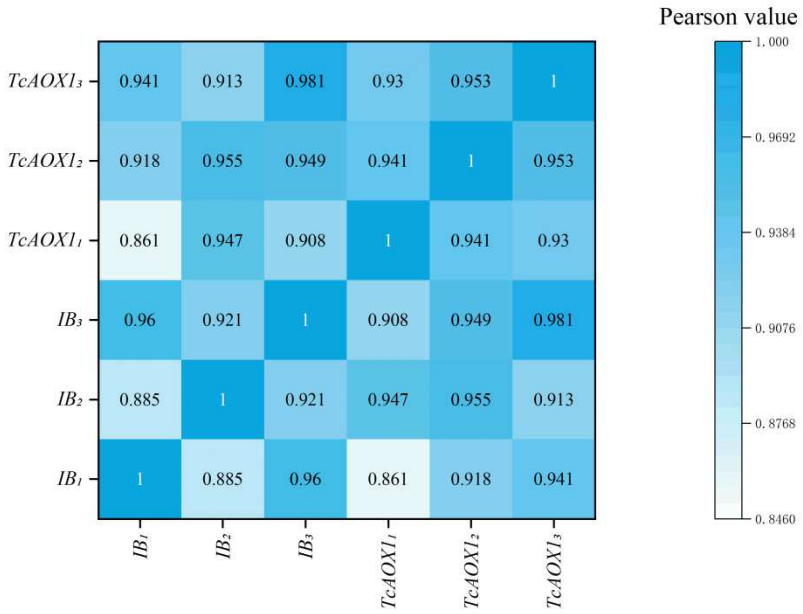


Fig. 2. Sample correlation analysis. The x- and y-axes represent the three biological replicate samples and experimental groups, respectively. The color intensity and numerical values within each square indicate the squared Pearson correlation coefficient (R^2) between sample pairs. As shown in the figure, all pairwise R^2 values exceeded 0.7, indicating high consistency and reliability among biological replicates, and confirming that the RNA-Seq data generated in this study are of sufficient quality for subsequent statistical analyses.

Functional Annotation of Differentially Expressed Genes

Gene Ontology (GO) and Kyoto Encyclopedia of Genes and Genomes (KEGG) enrichment analyses were performed to annotate the functions and pathways of the differentially expressed genes (DEGs). The GO annotation classified the DEGs into three main categories: biological process, cellular component, and molecular function, which were further subdivided into 17 GO terms. Among these, the most enriched term was catalytic activity, which mainly included genes encoding *serine protease P145, serine protease P147*, *serine protease P41*, and *carboxypeptidase A* (Table 2). Notably, the gene encoding *carboxypeptidase A* was also enriched in the cellular process category (Fig. 3A). In the KEGG enrichment analysis, the DEGs were enriched across five pathway categories, namely cellular processes, environmental information processing, human diseases, metabolism, and organismal systems, with the metabolism pathway further divided into two sub-branches (Fig. 3B). A total of 15 DEGs were enriched, as shown in Fig. 4, and detailed information is provided in Table S4. A clustering heatmap of DEG expression levels revealed similarities and differences between two biological replicates from the IB control and ds*TcAOX1*-treated groups (Fig. 4).

Table 2. Differentially expressed genes enriched in the catalytic activity pathway.

Gene ID	log2(*TcAOX1*/IB)	Regulation (*TcAOX1*/IB)	Gene description	Qvalue (*TcAOX1* / IB)
LOC658535	3.33181080177079	Up	Gram-negative bacteria binding protein 1	0.002169859013929
LOC660388	1.3619863928916	Up	Lysine ketoglutarate reductase	0.0252814024404897
LOC662042	1.42570863028244	Up	N-acetyl-alpha-glucosaminidase	0.0076720756590124
LOC656097	-1.644515788	Down	chymotrypsin-like proteinase 5A	0.0316943261738922
LOC656185	-2.690519263	Down	chymotrypsin-like proteinase 5B precursor	0.0032736894445065
LOC656929	-2.21928786	Down	carboxypeptidase A	0.042971753130695
LOC661254	-1.381481183	Down	serine protease P41	0.0193626042316782
LOC662396	-1.067310297	Down	hypothetical protein	0.0281877303971031

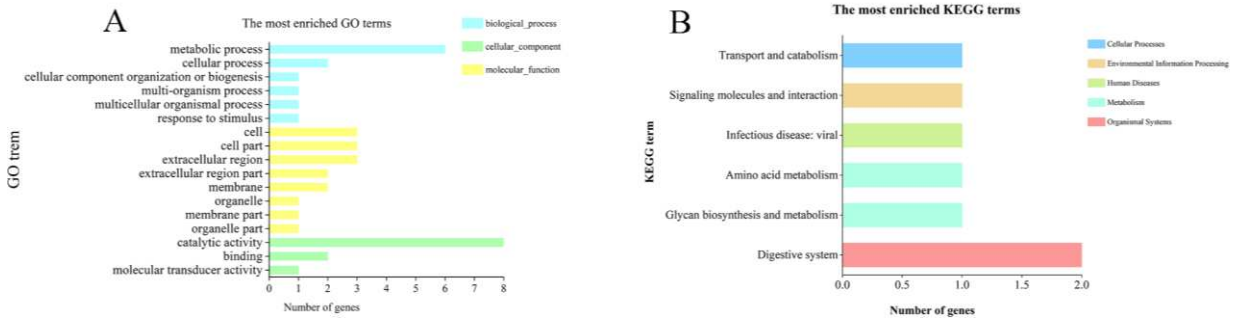


Fig. 3. Histogram of Gene Ontology (GO) classification of differentially expressed genes (DEGs) (A) and histogram of KEGG pathway classification of DEGs (B). DEGs were enriched in the ds*TcAOX1*-injected group compared with the IB-injected group. The GO annotation classified DEGs into three main functional categories: biological process, cellular component, and molecular function, each containing subcategories at various levels. The horizontal axis represents the number of genes annotated to each GO term, and the vertical axis represents the GO functional categories (A). In the KEGG enrichment analysis, the metabolic pathways involving DEGs were categorized into five major branches: cellular processes, environmental information processing, human diseases, metabolism, and organismal systems, with further sub-classifications. The horizontal axis represents the number of genes annotated to each KEGG pathway category, and the vertical axis represents the KEGG pathway categories (B).

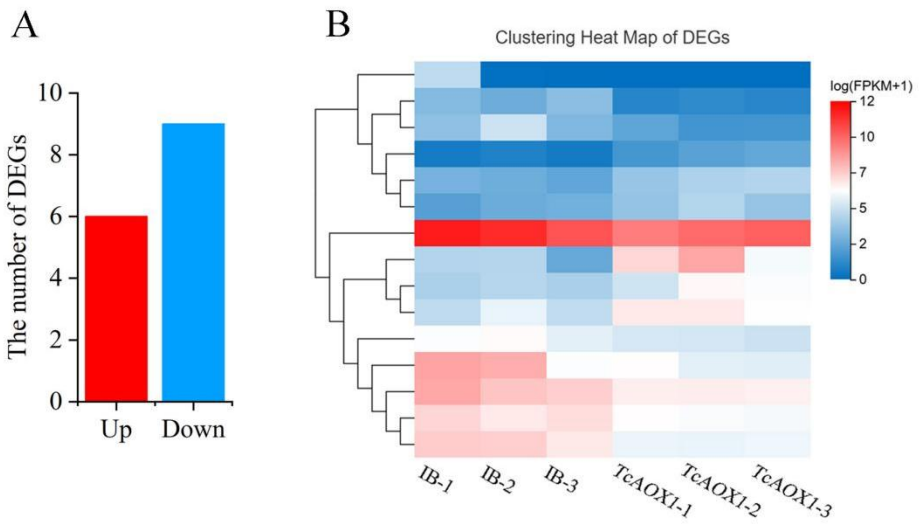
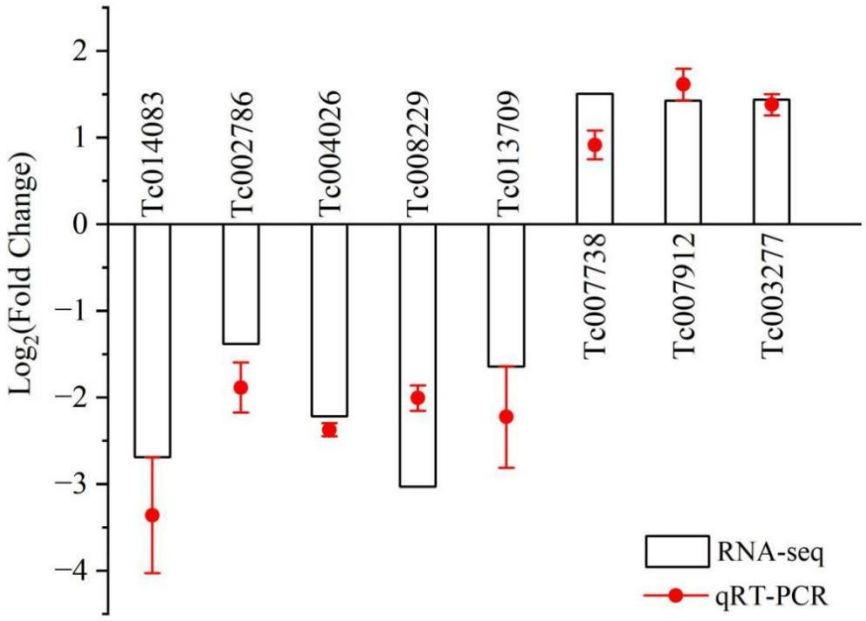


Fig. 4. Overview of differentially expressed genes (DEGs) (A) and clustering heatmap of DEGs (B). (A) Number of DEGs between the ds*TcAOX1*-injected and IB-injected groups. The horizontal axis represents upregulation and downregulation, and the vertical axis represents the number of DEGs. (B) Clustering heatmap of DEG expression levels. Rows represent individual genes, and columns represent comparisons between the *TcAOX1*-treated and IB control groups. Samples were grouped based on the similarity of transformed log10 gene expression values, with different colors indicating varying degrees of differential expression.

QPCR Validation of RNA-Seq Data

To validate the accuracy of the RNA-Seq data, we performed qPCR on five downregulated and three upregulated genes. The qPCR results were consistent with the RNA-Seq data, with minor variations within an acceptable range (Fig. 5). Collectively, these results confirmed the reliability of the RNA-Seq data.



244

245 Fig. 5. Comparison of RNA-Seq data and qPCR results for selected genes. The horizontal axis represents the gene
246 symbols, and the vertical axis represents the $\log_2$(fold change) relative to the control group (IB-injected group).
247 Transcript levels of *Tcrps3* (*ribosomal protein S3*) in the IB-injected group were used as the reference for
248 normalization. Data are presented as mean ± SE, n = 3.

249

Discussion

In insects, aldehyde oxidases (AOXs) serve two primary functions: involvement in the detoxification of xenobiotics and the degradation of odorant signals. Studies have suggested that AOXs have diverged into two major evolutionary branches: one branch may have originated from ancestral groups and is presumed to be associated with the degradation of plant volatiles, whereas the other branch appears to be more specialized in the degradation of sex pheromones(Ricardo, Ana, Leonela, & Herbert, 2022).Previous studies have shown that knockdown of *TcAOX1* expression in *T. castaneum* leads to a subsequent decrease in oviposition rate(Yonglei Zhang et al., 2022).In this study, RNA interference (RNAi) was performed in *T. castaneum*. The results showed that the expression level of *TcAOX1* was significantly reduced following injection of ds*TcAOX1* compared with the control group. Microinjection of dsRNA into the insect hemocoel is one of the most widely used and reliable RNAi methods in current insect gene functional studies(Li, Wang, Wang, Ma, & Hua, 2013),By microinjection, dsRNA can effectively bypass physiological barriers such as the insect gut and be delivered directly into the hemolymph, thereby triggering a systemic RNAi response more efficiently(Zheng et al., 2025).

To further elucidate how *TcAOX1* participates in the reproduction of *T. castaneum*, total RNA was extracted from late-instar larvae at five days post-injection of ds*TcAOX1*, along with that from the IB-injected control group, and subjected to RNA-Seq. Through analysis of the RNA-Seq data, a total of 15 differentially expressed genes (DEGs) were ultimately identified, followed by KEGG and GO enrichment analyses. In the catalytic activity GO term, eight genes were enriched, including those encoding serine protease P145, serine protease P147, serine protease P41, and carboxypeptidase A, among others (Table 2).Knockdown of *TcAOX1* expression resulted in the downregulation of carboxypeptidase genes. In comparison, when adults of *Ophraella communa* were fed with dsRNA targeting the *OcCpb* gene, their oviposition significantly decreased relative to the control group(G. Chen et al., 2023).In addition, RNAi-mediated knockdown of a carboxypeptidase gene highly expressed in the male accessory gland of *Grapholita molesta* resulted in a significant reduction in male fertility(Cheng et al., 2025),This suggests that *TcAOX1* may positively regulate carboxypeptidase genes, thereby participating in the regulation of reproduction in *T. castaneum*. Furthermore, the expression of serine protease genes also decreased following the knockdown of *TcAOX1*. Previous studies have shown that RNAi-mediated knockdown of *serine protease P145* impairs embryonic development,

resulting in reduced body segments and shortened appendages. Likewise, knockdown of *serine protease P147* affects eclosion, leading to a range of phenotypic defects, including irregular muscle distribution in embryos, lack of embryonic cuticle, low hatching rate, absence of the dorsal ridge, reduced mouthpart size, malformed head appendages, loss of antennae, and larvae lacking a distinct cuticle(Dönitz et al., 2015).Functional disruption of the ovary-serine protease gene *PxOsp* in the diamondback moth, *Plutella xylostella*, results in complete female sterility, a significant reduction in egg production, failure of the remaining eggs to hatch, and severe defects such as obvious cracking of the eggshell(Dönitz et al., 2015).The serine protease encoded by *BmSer1* in the silkworm, *Bombyx mori*, is essential for male reproduction in lepidopteran insects(X. Xu et al., 2022).Disruption of *Ser2*, which encodes a seminal serine protease, results in male sterility in the silkworm (*Bombyx mori*) and the diamondback moth (*Plutella xylostella*), an important agricultural pest(Xia Xu et al., 2020).Together, these findings suggest that *TcAOX1* may be involved in regulating reproduction in *T. castaneum* through modulating the expression of serine protease genes. Additionally, among the other differentially expressed genes between the *TcAOX1*-treated and IB control groups, the gene encoding the cuticular protein *cuticlin-2* was significantly downregulated, suggesting its potential involvement in the reproductive process of *T. castaneum*. In insects, cuticular proteins are critical components of the integument, epidermis, and the inner lining of the reproductive ducts(Mercati, Giglio, Brandmayr, Lupetti, & Dallai, 2024; Qi & Liu, 2025).Cuticular proteins are essential for the development of reproductive structures. For instance, deficiency of the cuticular protein gene *LmCP8* in the migratory locust, *Locusta migratoria*, directly affects the structural development of the ovipositor valves, thereby leading to oviposition defects(Zhao et al., 2022).The *Cpr21L* gene in the brown planthopper (*Nilaparvata lugens*) encodes a cuticular protein. When *Cpr21L* was silenced by the research team, the fecundity of female adults decreased significantly by 50.1% compared with the control group(T. Chen et al., 2023).Furthermore, studies have shown that some cuticular protein (CP) genes encoded in the genome of the brown planthopper are essential for nymphal development, oviposition, or embryonic development.(Pan et al., 2018).Therefore, the *cuticlin-2* gene may serve as a key mediator through which *TcAOX1* participates in the regulation of reproduction in *T. castaneum*. Collectively, these findings suggest that *TcAOX1* may influence reproduction in *T. castaneum* by modulating the expression of multiple genes, including *carboxypeptidase A (CPA)*, *cuticlin-2*, *serine protease P145*, and *serine protease P147*.

Conclusion

In this study, RNA interference (RNAi) was first applied to late-instar larvae of *T. castaneum* to knock down *TcAOX1* expression, with both control and *TcAOX1*-treated groups each comprising three biological replicates. Subsequently, RNA sequencing (RNA-Seq) was performed to identify differentially expressed genes (DEGs) between the *TcAOX1*-treated and IB control groups. Among the identified DEGs, the *cuticlin-2* gene, which encodes a cuticular protein, was found to be potentially involved in the reproductive process of *T. castaneum*. Through Gene Ontology (GO) and Kyoto Encyclopedia of Genes and Genomes (KEGG) enrichment analyses for functional and pathway annotation, our results suggest that *TcAOX1* may influence reproduction in *T. castaneum* by modulating the expression of *cuticlin-2*, as well as other genes enriched in GO terms such as catalytic activity and cellular component, including *carboxypeptidase A (CPA)*, *serine protease P145*, and *serine protease P147*. Collectively, this study implies that *TcAOX1* is involved in the regulation of reproduction in *T. castaneum*, providing new insights for the development of environmentally friendly pest management strategies against this species.

Acknowledgements

This research was supported by the Natural Science Foundation of Henan Province (252300423543).

Declaration of interest

The authors declare that they have no known competing financial interests or personal relationships that could have appeared to influence the work reported in this paper.

Funding Declaration

This work was supported by the Natural Science Foundation of Henan Province (Grant No. 252300423543).

Clinical trial numbe: not applicable.

References

Barun Mangang, I., Loganathan, M., Malemnganbi, S., & Induja, C. (2025). Pheromone traps: analysing the factors helpful in mitigating the use of chemical insecticides for sustainable practices in storing food product commodities. *Sustainable Food Technology, 4*(1), 153-163. doi:https://doi.org/10.1039/d5fb00215j

Chen, G., Gao, X., Zhang, Y., Ma, C., Ma, W., & Zhou, Z. (2023). The carboxypeptidase B and carbonic anhydrase genes play a reproductive regulatory role during multiple matings in *Ophraella communa*. *Frontiers in Molecular Biosciences, 10*, 1095645. doi:10.3389/fmolb.2023.1095645

Chen, T., Jiao, Q., Ye, C., Wu, J., Zheng, Y., Sun, C., . . . Yu, X. (2023). A Novel Cuticular Protein-like Cpr21L Is Essential for Nymph Survival and Male Fecundity in the Brown Planthopper. *International Journal of Molecular Sciences, 24*(3): 2163. doi:10.3390/ijms24032163

Chen, X., Xu, K., Yan, X., Chen, C., Cao, Y., Wang, Y., Yang, W. (2018). Characterization of a β-N-acetylglucosaminidase gene and its involvement in the development of Lasioderma serricorne (Fabricius). *Journal of Stored Products Research, 77*: 156-165. doi:https://doi.org/10.1016/j.jspr.2018.04.012

Chen, Y., Wang, J., Liu, Z., Wang, X., Li, X., & Shan, G. (2018). A simple and versatile paper-based electrochemiluminescence biosensing platform for hepatitis B virus surface antigen detection. *Biochemical Engineering Journal, 129:* 1-6. doi:https://doi.org/10.1016/j.bej.2017.10.012

Cheng, J., Wei, W., Zhang, Y., Zhu, F., Shen, Z., Li, X., Ma, R. (2025). Male accessory gland-derived carboxypeptidase B regulates sperm activation in the spermatophores of Grapholita molesta. *Journal of Insect Physiology, 165*: 104858. doi:https://doi.org/10.1016/j.jinsphys.2025.104858

Chertemps, T., François, A., Durand, N., Rosell, G., Dekker, T., Lucas, P., & Maïbèche-Coisne, M. (2012). A carboxylesterase, Esterase-6, modulates sensory physiological and behavioral response dynamics to pheromone in Drosophila. *Bmc Biology, 10*: 56. doi:10.1186/1741-7007-10-56

Choo, Y.-M., Pelletier, J., Atungulu, E., & Leal, W. S. (2013). Identification and Characterization of an Antennae-Specific Aldehyde Oxidase from the Navel Orangeworm. *Public Library of Science, 8*(6): e67794. doi:10.1371/journal.pone.0067794

Dönitz, J., Schmitt-Engel, C., Grossmann, D., Gerischer, L., Tech, M., Schoppmeier, M., Bucher, G. (2015). iBeetle-Base: a database for RNAi phenotypes in the red flour beetle *Tribolium castaneum*. *Nucleic Acids Research, 43*(Database issue): D720-725. doi:10.1093/nar/gku1054

Gao, S., Guo, M., Zhang, E., Yi, Z., Liu, K., Xue, S., . . . Zhang, K. (2025). RNA-seq analysis combined with insecticidal efficacy assays reveal the insecticidal molecular mechanism of benzaldehyde against *Tribolium castaneum*. *Genomics, 117*(6): 111128. doi:https://doi.org/10.1016/j.ygeno.2025.111128

Gao, S., Liu, K., Xue, S., Zhou, C., Zhang, G., Guo, M., & Cao, Y. (2025). RNA sequencing analysis uncovers the role of aldehyde oxidase *TcAOX2* in regulating toxic substance susceptibility in the red flour beetle, *Tribolium castaneum*. *Journal of Asia-Pacific Entomology, 28*(1): 102351. doi:https://doi.org/10.1016/j.aspen.2024.102351

Gao, S., Lu, R., Zhang, Y., Sun, H., Li, S., Zhang, K., & Li, R. (2021). Odorant binding protein C12 is involved in the defense against eugenol in *Tribolium castaneum. Pesticide Biochemistry and Physiology, 179*: 104968. doi:https://doi.org/10.1016/j.pestbp.2021.104968

Garattini, E., Fratelli, M., & Terao, M. (2009). The mammalian aldehyde oxidase gene family. *Hum Genomics, 4*(2): 119-130. doi:10.1186/1479-7364-4-2-119

Godoy, R., Arias, I., Venthur, H., Quiroz, A., & Mutis, A. (2022). Characterization of Two Aldehyde Oxidases from the Greater Wax Moth, *Galleria mellonella* Linnaeus. (Lepidoptera: Pyralidae) with Potential Role as Odorant-Degrading Enzymes. *Insects, 13*(12): 1143. doi:10.3390/insects13121143

Kim, D., Langmead, B., & Salzberg, S. L. (2015). HISAT: a fast spliced aligner with low memory requirements. *Nature Methods, 12*(4): 357-360. doi:10.1038/nmeth.3317

Langmead, B., & Salzberg, S. L. (2012). Fast gapped-read alignment with Bowtie 2. *Nature Methods, 9*(4): 357-359. doi:10.1038/nmeth.1923

Li, J., Wang, X. P., Wang, M. Q., Ma, W. H., & Hua, H. X. (2013). Advances in the use of the RNA interference technique in Hemiptera. *Insect Science, 20*(1): 31-39. doi:10.1111/j.1744-7917.2012.01550.x

Love, M. I., Huber, W., & Anders, S. (2014). Moderated estimation of fold change and dispersion for RNA-seq data with DESeq2. *Genome Biology, 15*(12): 550. doi:10.1186/s13059-014-0550-8

Mercati, D., Giglio, A., Brandmayr, P., Lupetti, P., & Dallai, R. (2024). The spermatheca ultrastructure of the ground beetle Clinidium canaliculatum (Costa) (Carabidae, Rhysodinae). *Micron, 187*:

103721. doi:10.1016/j.micron.2024.103721
Pan, P. L., Ye, Y. X., Lou, Y. H., Lu, J. B., Cheng, C., Shen, Y., Zhang, C. X. (2018). A comprehensive omics analysis and functional survey of cuticular proteins in the brown planthopper. *Proceedings of the National Academy of Sciences of the United States of America,* 115(20): 5175-5180. doi:10.1073/pnas.1716951115
Pelletier, J., Bozzolan, F., Solvar, M., François, M.-C., Jacquin-Joly, E., & Maïbèche-Coisne, M. (2007). Identification of candidate aldehyde oxidases from the silkworm Bombyx mori potentially involved in antennal pheromone degradation. *Gene, 404*(1): 31-40. doi:https://doi.org/10.1016/j.gene.2007.08.022
Qi, H., & Liu, T. (2025). Cuticular proteins: Essential molecular code for insect survival. *Insect Biochemistry and Molecular Biology,* 184: 104402. doi:10.1016/j.ibmb.2025.104402
Ricardo, G., Ana, M., Leonela, C. P., & Herbert, V. (2022). Genome-Wide Identification of Aldehyde Oxidase Genes in Moths and Butterflies Suggests New Insights Into Their Function as Odorant-Degrading Enzymes. *Frontiers in Ecology and Evolution,* 10: 823119 doi:10.3389/fevo.2022.823119
Rybczynski, R., Reagan, J., & Lerner, M. R. (1989). A pheromone-degrading aldehyde oxidase in the antennae of the moth Manduca sexta. *J Neurosci, 9*(4): 1341-1353. doi:10.1523/jneurosci.09-04-01341.1989
Rybczynski, R., Vogt, R. G., & Lerner, M. R. (1990). Antennal-specific pheromone-degrading aldehyde oxidases from the moths Antheraea polyphemus and Bombyx mori. *Journal of Biological Chemistry, 265*(32): 19712-19715. doi:https://doi.org/10.1016/S0021-9258(17)45430-5
Terao, M., Romão, M. J., Leimkühler, S., Bolis, M., Fratelli, M., Coelho, C., Garattini, E. (2016). Structure and function of mammalian aldehyde oxidases. *Archives of Toxicology, 90*(4): 753-780. doi:10.1007/s00204-016-1683-1
Wang, M.-M., He, M., Wang, H., Ma, Y.-F., Dewer, Y., Zhang, F., & He, P. (2021). A candidate aldehyde oxidase in the antennae of the diamondback moth, Plutella xylostella (L.), is potentially involved in the degradation of pheromones, plant-derived volatiles and the detoxification of xenobiotics. *Pesticide Biochemistry and Physiology, 171*: 104726. doi:https://doi.org/10.1016/j.pestbp.2020.104726
Xu, W., & Liao, Y. (2017). Identification and characterization of aldehyde oxidases (AOXs) in the cotton bollworm. *The Science of Nature, 104*. doi:10.1007/s00114-017-1515-z
Xu, X., Wang, Y., Bi, H., Xu, J., Liu, Z., Niu, C., . . . Huang, Y. (2020). Mutation of the seminal protease gene, serine protease 2, results in male sterility in diverse lepidopterans. *Insect Biochemistry and Molecular Biology, 116*: 103243. doi:https://doi.org/10.1016/j.ibmb.2019.103243
Xu, X., Wang, Y., Chen, J., Du, X., Yao, L., Xu, J., . . . Wang, Y. (2022). Mutation of Serine protease 1 Induces Male Sterility in Bombyx mori. *Front Physiol,* 13: 828859. doi:10.3389/fphys.2022.828859
Zhang, Y., Yang, Y., Shen, G., Mao, X., Jiao, M., & Lin, Y. (2020). Identification and Characterization of Aldehyde Oxidase 5 in the Pheromone Gland of the Silkworm (Lepidoptera: Bombycidae). *Journal of Insect Science, 20*(6): 31. doi:10.1093/jisesa/ieaa132
Zhang, Y., Zhang, J., Li, D., Sun, H., Lu, R., Yin, S., Gao, S. (2022). Aldehyde oxidases mediate plant toxicant susceptibility and fecundity in the red flour beetle, *Tribolium castaneum*. *Bulletin of Entomological Research,* 112(5): 656-666. doi:10.1017/S0007485322000049
Zhao, X., Su, Y., Shao, T., Fan, Z., Cao, L., Liu, W., & Zhang, J. (2022). Cuticle protein gene LmCP8 is involved in the structural development of the ovipositor in the migratory locust Locusta migratoria. *Insect Biochemistry and Molecular Biology, 31*(6): 747-759. doi:10.1111/imb.12801
Zheng, H., Hua, M., Jiang, M., Jiang, C., Xi, Y., Deng, J., . . . Zhou, S. (2025). Transgenic expression of mAChR-C dsRNA in maize confers efficient locust control. *Plant Commun, 6*(5): 101316. doi:10.1016/j.xplc.2025.101316

Table S4. Differentially expressed genes (DEGs)

GeneID	log2 (*TcAOX1*/IB)	Regulation (*TcAOX1*/IB)	Qvalue (*TcAOX1*/IB)	Protein	Phenotype after RNAiof DEGs in *T.castaneuma*
103312581	-1.080210116	Down	0.003273689444506 5	uncharacterized	
107398282	-1.652674592	Down	3.99442109119087E-6	uncharacterized	
662396	-1.067310297	Down	0.028187730397103 1	hypothetical protein	Incomplete eclosion and increased hatching rate
655120	-3.031291506	Down	3.33243851640319E-5	cuticlin-2	Increased hatching rate
656097	-1.644515788	Down	0.031694326173892 2	serine protease P145	Increased hatching rate; impaired embryonic development
656185	-2.690519263	Down	0.003273689444506 5	serine protease P147	Incomplete eclosion; impaired embryonic development
661254	-1.381481183	Down	0.019362604231678 2	serine protease P41	Increased hatching rate
664115	-22.9122554	Down	1.40724133504725E-5	probable serine/threonine-protein kinase tsuA	
656929	-2.21928786	Down	0.042971753130695	carboxypeptidase A	Incomplete eclosion and increased hatching rate
100141947	1.50146139625402	Up	0.043442384859820 9	attacin 2	
103312224	1.43456790209772	Up	0.007672075659012 4	uncharacterized	
103314786	2.56706607588605	Up	8.01799544808639E-6	leucine-rich repeat-containing protein egg-6-like	
658535	3.33181080177079	Up	0.002169859013929	Gram-negative bacteria binding protein 1	
660388	1.3619863928916	Up	0.025281402440489 7	Lysine ketoglutarate reductase/saccharopine dehydrogenase	
662042	1.42570863028244	Up	0.007672075659012 4	N-acetyl-alpha-glucosaminidase	